PHYSICAL REVIEW C VOLUME 19, NUMBER 3 MARCH 1979

Isotopic mass dispersion discontinuity in various fission processes and its interpretation as a neutron shell effect

R. K. Tokay and M. Talât-Erben
Department of Physical Chemistry, Faculty of Chemical Engineering, Technical University of Istanbul, Istanbul, Turkey
(Received 24 July 1978)

The isotopic dispersions have been calculated for fission processes listed in the Introduction below by using recommended fission yield data. Those dispersions in which the neutron numbers of isotopes lying in the vicinity of the most probable mass fit a strong shell have been found to be pronouncedly discontinuous; the discontinuity is proved to occur exactly at the most probable mass. The influence of neutron shells on mass dispersion with special reference to discontinuity is discussed on the basis of shell correction vs deformation and neutron number reported by Wilkins, Steinberg, and Chasman. In discontinuous dispersions on the narrower branch lie the isotopes fitting the strong spherical and deformed neutron shells. Apart from recommended data, the relative isotopic fragment yields predicted by the Wilkins-Steinberg model for the complementary pairs z = 50-42, 51-41, 54-38, and 56-36, in thermal-neutron fission of ^{235}U have also been used to calculate the corresponding dispersions. These have been found to be in good agreement with those calculated from recommended data, and discontinuities were observed, in general, wherever expected.

[NUCLEAR REACTIONS, FISSION ^{232}Th, ^{233}U, ^{235}U, ^{238}U, ^{239}Pu, ^{252}Cf; calculated isotopic mass dispersions from recommended yields and Wilkins-Steinberg model. Discontinuity as neutron-shell effect.]

I. INTRODUCTION

In low-energy fission (excitation energy ≤ 14 MeV) the mass dispersion, i.e., the formation probability of isotopic products as a function of mass number A can be represented adequately by a normalized Gaussian $P_Z(A) = (\pi c)^{-1/2}\exp[-(A-A_p)^2/c]$, where $P_Z(A)$ is the independent isotopic fractional product yield, A_p is the most probable mass, and c is the width parameter. However, it was shown[1] that in thermal-neutron-induced fission of ^{235}U the isotopic mass dispersion curves for many isotopes are discontinuous at A_p, the two branches consisting of two different Gaussians. This observation and the large amount of fission yield data accumulated heretofore and compiled recently[2,3,4] for various fission processes stimulated us to calculate the mass dispersion and investigate the discontinuity in all fission processes for which selected data were available; namely, spontaneous, ^{252}Cf; thermal-neutron-induced, ^{233}U, ^{235}U, and ^{239}Pu; fission-spectrum-neutron-induced, ^{232}Th, ^{235}U, and ^{238}U; 14 MeV-neutron-induced, ^{235}U and ^{238}U.

Some of the calculated width parameters and the neutron contents of the corresponding products clearly indicate that the neutron shells are responsible for the discontinuity.

II. CALCULATIONS

A. Isotopic mass dispersion parameters

In order to obtain the isotopic mass dispersion it is necessary to calculate $P_Z(A)$ for each Z. These calculations are based on the recommended fission yields compiled by Meek and Rider[2] and by Wolfsberg[3]. The recommended independent yields $y(Z,A)$ reported by Meek and Rider were used to calculate the mass dispersions for the above-mentioned fission processes, except for spontaneous fission of ^{252}Cf in which case enough recommended data are not reported, and Erten's[4] data were used. The $P_Z(A)$ values are obtained by dividing each $y(Z,A)$, by $y(Z)=\sum_A y(Z,A)$.

For comparison, Wolfsberg's independent isobaric fractional yields $P_A(Z)$ were also used to calculate the mass dispersions for the same processes, except the thermal-neutron-induced fission of ^{239}Pu and spontaneous fission of ^{252}Cf. Using these $P_A(Z)$ values along with the cumulative isobaric chain yields $y(A)$ of Meek and Rider, a Weierstrass transform[5] was performed to obtain the isotopic chain yields $y(Z)=\sum_Z y(A)P_A(Z)$. The sought $P_Z(A)$ values were finally obtained by normalization: $P_Z(A)=y(Z,A)/y(Z)$.

The $P_Z(A)$ values thus obtained were treated by two different techniques to calculate the Gaussian

parameters A_p and c.

Presuming that for a given Z two different Gaussians are operative for mass numbers smaller and greater than the most probable mass, respectively, a smooth dispersion curve was constructed beforehand to read off an approximate A_p value, $(A_p)_{approx}$.

(1) *Calculation based on the "minimum systematic variance"*[6]: The Gaussian distribution can be expressed explicitly with respect to A_p. This expression allows calculation of various A_p values by inserting arbitrary c values. If $\bar{A}_p$ is the arithmetic mean of the A_p values calculated for each arbitrary c, then the sum of squared systematic errors, $v = \sum[A_p - \bar{A}_p(c)]^2$, committed by inserting arbitrary values for c will be a minimum, v_{min}, for the correct value of c corresponding to the best fit. The method has been applied to data lying on either side of $(A_p)_{approx}$, separately. On the average six data were available for each branch.

To check the Gaussian nature of the dispersion, $\ln P_Z(A)$ was plotted against $(A - A_p)^2$, where A_p is the $\bar{A}_p$ value corresponding to v_{min}. This plot must be linear if the dispersion is truly Gaussian.

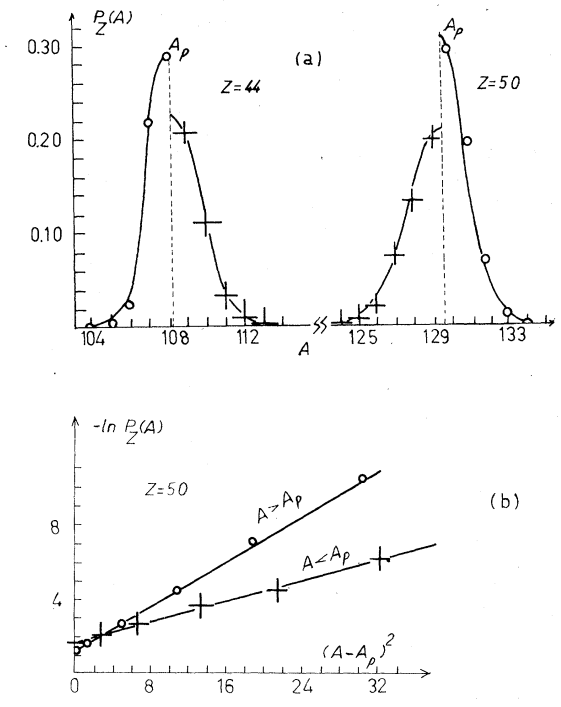

FIG. 1. (a) Isotopic mass dispersion for the complementary pairs $Z = 44$ and 50 in thermal fission of ^{239}Pu, calculated from Meek-Rider data (Ref. 2). As seen, two different Gaussian curves apply on either side of the most probable mass A_p. Note the mirror-image relationship of the corresponding branches. (b) Logarithmic diagram indicating that the two branches are Gaussian.

Two distinct intersecting straight lines are obtained wherever the dispersion is significantly discontinuous *and* Gaussian on both sides of A_p (Fig. 1).

(2) *Alternative calculation based on smoothing by truncated Fourier collocation*[7]: The Fourier analysis makes it possible to treat the isotopic mass dispersion without postulating in advance its Gaussian character. On the contrary, the Gaussian feature is deduced as a property of the Fourier collocation.[7,8] Three collocation expressions have been evaluated in each case. First, the fact that, due to discontinuity, the data on either side of A_p do not lie on a single curve is omitted, and a "hybrid" collocation expression is calculated. A second collocation sum is evaluated by using the data for mass numbers smaller than A_p, and a third one from the data for mass numbers greater than A_p. In continuous cases the respective numerical coefficients of the three collocations are found to be very nearly the same (99% correlation or over), as required by the well-known theorem which asserts that a function can be expanded in a Fourier series in a unique way. On the other hand, if discontinuity is present, the three collocation expressions differ considerably. In both cases the Gaussian character of the branches can be checked by plotting again $\ln P_Z(A)$ vs $(A - A_p)^2$. Excellent agreement has been found between the results calculated by the two techniques.

III. RESULTS AND DISCUSSION

The calculated Gaussian parameters c and A_p lead to the following conclusions:

(1) In the above-mentioned fission processes, except for spontaneous fission of ^{252}Cf, most of the isotopic mass dispersion curves were found to be discontinuous at the most probable mass, where the dispersion is Gaussian on either side except in some rare cases in which one branch is non-Gaussian. In discontinuous dispersions the difference between the width parameters is larger than 0.8 (Figs. 1, 2, and 3).

(2) Discontinuity in isotopic mass dispersion in spontaneous fission of ^{252}Cf was observed only for the complementary isotopic products $Z = 50$ and 48, where the two branches of the dispersion are Gaussian. The common absence of discontinuity in this process is rather unexpected and in contradiction with the universal character of neutron-shell effects which will be shown shortly to be the cause of the discontinuity. This behavior could possibly be accounted for by some oversmoothing inherent to Erten's[4] data.

(3) Even in cases in which distinctly different width parameters were found, almost the same

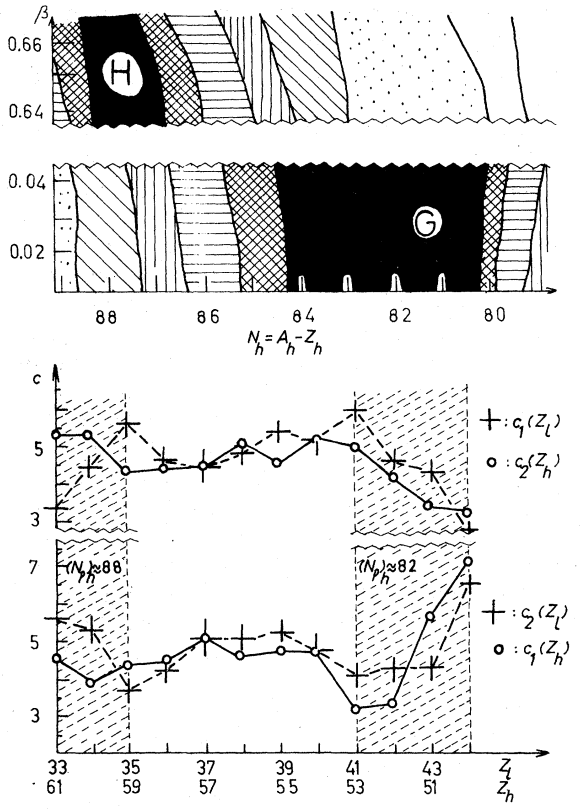

FIG. 2. *Lower part*: Width parameters for the opposite branches of the dispersion in thermal fission of ^{239}Pu, as a function of complementary charge numbers Z_l and Z_h. Note that a larger band corresponds to the stronger spherical shell region around $N = 82$. *Upper part*: A portion of the neutron-shell correction vs β and N surface (Ref. 12) which falls in the region covered by the lower diagram is reproduced for comparison. Note the excellent matching of the shells and the bands.

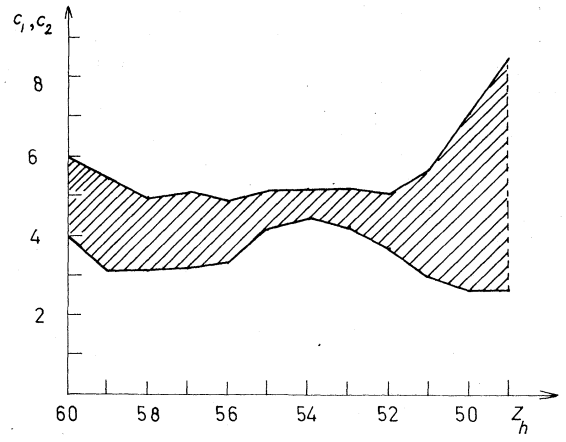

FIG. 3. The width parameters of the same dispersion as a function of Z for all fission processes considered. The narrow region in the middle corresponds to continuous dispersions ($\Delta c \leq 0.8$), while the two broad regions at the ends occur at the two neutron shells G and H of Fig. 2.

A_p values (99% correlation or over) were obtained separately from the two branches of the dispersion, a fact indicating that the discontinuity occurs exactly at A_p.

(4) Either side of a discontinuous dispersion is one half of a sharper or a broader Gaussian, the other half of which is to be found as its mirror image in the dispersion corresponding to the complementary charge. In other words, roughly the same c value characterizes the opposite (or symmetric) branches of dispersion curves with complementary charge numbers [Figs. 1(a) and 2].

(5) With a very few exceptions the discontinuous dispersions are found in the following regions: $49 \leq Z \leq 54$, and at $Z = 59$ and 60 for the heavy group, and $41 \leq Z \leq 43$, and at $Z = 33$ for the light group. Outside these regions, the discontinuity, if any, is negligible ($\Delta c < 0.8$) so that the dispersion can adequately be represented by a single Gaussian (Fig. 3).

(6) It is interesting to compare the widths of the Gaussian halves of discontinuous dispersions with the corresponding most probable neutron numbers, $N_p = A_p - Z$ (Table I, II, and III). The sharper half (a smaller c) corresponds to higher yields for products in the vicinity of N_p. A close inspection of Table I, and a consideration of the average neutron numbers emitted by the fragments $\bar{\nu}$ show that *in all discontinuous dispersions the products lying near the maximum of the sharper branch are formed from fragments containing as many neutrons as required by the strong neutron shell at $N = 82$.*

In column $Z = 50$, where $\bar{\nu} = 0.55$,[8] N_p varies from 78.5 to 81.5, and the products born in the strong neutron-shell region are found to lie on the right half ($N < N_p$) of the dispersions, giving rise to very sharp Gaussian branches, as expected. For all non-Gaussian branches the $P_Z(A)$ values in the vicinity of A_p are considerably smaller than the corresponding values on the opposite branches.

In column $Z = 51$, where $\bar{\nu} = 0.80$, N_p has higher values than those of column $Z = 50$, approaching $N = 82$. Except for spectrum-neutron fission of ^{232}Th and ^{238}U, $N_p < 82$ and the right halves of the dispersions are sharper than the branches to the left of N_p. In spectrum-neutron fission of ^{232}Th, $N_p = 81.5$ for $Z = 51$, and the dispersion is representable practically by a single sharp Gaussian ($c_1 = 3.5$, $c_2 = 3.8$). This can be interpreted by taking into account both the neutron emission prob-

TABLE I. A comparison of the Gaussian widths c_1 and c_2 for the left and right halves of the isotopic mass dispersions, respectively, with the most probable neutron numbers, $N_p = A_p - Z$, in the strong spherical neutron-shell region at $N \sim 82$. Based on the Meek-Rider report (Ref. 2).

Fissioning system		$Z=50$			$Z=51$			$Z=52$			$Z=53$		
		c_1	N_p	c_2	c_1	N_p	c_2	c_1	N_p	c_2	c_1	N_p	c_2
^{232}Th	(spectr.-neutron)	4.9	81	2.7	3.5	81.5	3.8	3.2	82	4.2			
^{233}U	(thermal)	7.0	79	3.1	5.4	80	3.6	5.0	81	4.5			
^{235}U	(thermal)	5.3	80.5	2.9	4.1	81	3.0	3.4	82	4.6	3.4	83	4.9
^{235}U	(spectr.-neutron)	n.G.[a]	80	3.0	5.2	81	3.6	3.1	82	4.3	3.5	83	4.7
^{235}U	(14 MeV)	n.G.	78.5	3.7	n.G.	79.5	3.9	4.5	80.5	4.5	3.3	81.5	5.7
^{238}U	(spectr.-neutron)	4.5	81.5	3.1	2.9	82	3.8	3.0	83	4.9			
^{238}U	(14 MeV)	6.8	80	3.3	n.G.	81	3.4	3.1	82	5.0			
^{239}Pu	(thermal)	7.0	79.5	3.3	5.6	80.5	3.4	3.3	81	4.2	3.2	82.5	5.0

[a] n.G. : non-Gaussian.

ability and the closeness of N_p to 82. Hence, the fragments formed in the strong neutron-shell region would be expected to raise also the formation probability of products to the right of N_p. This effect comes out more pronouncedly in the case of spectrum-neutron fission of ^{238}U, where $N_p = 82$ for $Z = 51$, showing a very sharp Gaussian half to the left of N_p, the right half being also considerably sharp ($c_1 = 2.9; c_2 = 3.8$).

The same reasoning applies to columns $Z = 52$ and $Z = 53$ where for the majority of the dispersions $N_p = 82$ and $\bar{\nu} \approx 1.0$. For dispersions where $N_p = 83$, the Gaussian branches representing isotopes with $N < N_p$ are always sharper than the opposite branches, again, as would be expected.

Here, it should be noted that Strutinsky's method,[9] which recently has been proved to be successful in describing various phenomena associated with nuclear deformation predicts deformed shells at different nucleon numbers in addition to the spherical one at $N = 82$. These shells are, in fact, relatively broad regions defined by the so-called magic numbers of nucleons and the related deformations.

Table II covers the discontinuous dispersions, where N_p ranges from 89.5 to 93.5. According to the above-mentioned argument, the sharp Gaussian branches for products with $N < N_p$ indicate the presence of a strong neutron shell near 89. Then, it appears that the shell effects operate at relatively broad regions around $N = 82$ and $N \approx 89$ (Figs. 2 and 3).

TABLE II. A comparison of the Gaussian widths c_1 and c_2 for the left and right halves of the isotopic mass dispersions, respectively, with the most probable neutron numbers, $N_p = A_p - Z$, in the strong deformed neutron-shell region at $N \approx 88$.

Fissioning system		Ref.	$Z=59$			$Z=60$		
			c_1	N_p	c_2	c_1	N_p	c_2
^{232}Th	(spectr.-neutron)	M-R[a]	3.2	90.5	5.0			
^{233}U	(thermal)	M-R	4.1	89.5	5.0			
		W[b]	4.2		4.9			
^{235}U	(thermal)	M-R	3.8	90	4.6			
		W	3.8		4.5			
^{235}U	(14 MeV)	M-R	3.5	89.5	6.6			
		W	3.3		5.8			
^{238}U	(spectr.-neutron)	M-R	3.5	92.5	5.0	4.0	93.5	5.9
		W	3.6		5.0	3.9		5.7
^{238}U	(14 MeV)	M-R	4.0	91	5.9	4.0	92	5.8
		W	3.9		5.7	3.9		5.5
^{239}Pu	(thermal)	M-R				3.9	92	5.4
		W				4.1		5.2

[a] M-R: Based on the Meek-Rider report (Ref. 2).
[b] W: Based on Wolfsberg's data (Ref. 3).

TABLE III. A comparison of the Gaussian widths c_1 and c_2 for the left and right halves of the isotopic mass dispersions, respectively, with the most probable neutron numbers, $N_p = A_p - Z$, for the complementary products for $Z = 50$ and 51.

Fissioning system		Ref.	c_1	$Z=41$ N_p	c_2	c_1	$Z=42$ N_p	c_2
^{232}Th	(spectr.-neutron)	M-R[b]	4.4	60.5	6.8		($Z=40$)	
						(3.2	59	6.8)
^{233}U	(thermal)	M-R				3.5	61	6.2
		W[c]				3.6		6.2
^{235}U	(thermal)	M-R				3.8	61.5	4.8
		W				3.7		5.1
^{235}U	(spectr.-neutron)	M-R	4.4	61	5.6	4.0	62	n.G.
		W	4.4		5.3	3.9		n.G.
^{235}U	(14 MeV)	M-R	4.3	61	6.8	3.9	62	n.G.
		W	4.1		n.G.[a]	4.1		n.G.
^{238}U	(spectr.-neutron)	M-R				3.6	63	5.1
		W				3.9		5.6
^{238}U	(14 MeV)	M-R	4.3	62	n.G.	4.5	63	8.3
		W	4.3		n.G.	4.5		8.3
^{239}Pu	(thermal)	M-R	5.9	61	4.1	(2.7	($Z=44$) 64	6.5)
		W	5.1		4.1	(3.7		5.3)

[a] n.G. : non-Gaussian.
[b] M-R : Based on the Meek-Rider report (Ref. 2).
[c] W: Based on Wolfsberg's data (Ref. 3).

The results concerning the complementary products for $Z = 50$ and 51 are given in Table III, where $\bar{\nu} \approx 3$. Here, the N_p values cover a broad region ranging from 59 to 64. If both the large number of evaporated neutrons and the complementarity to the fragments born in the strong spherical neutron-shell region centered at $N = 82$ be considered, a good agreement with statement (4) above can be noticed.

(7) In all fission processes investigated, A_p vs Z gives two almost parallel straight lines, one for the light group, another for the heavy group of fission products. The linearity of these functions and the fact that the most probable charge Z_p changes also nearly linearly with A, producing two almost parallel straight lines supports the bivariate normal distribution approach[10] to low-energy fission. A_p vs Z and Z_p vs A are the regression lines of the bivariate distribution and intersect at the projections $(\bar{A}_l, \bar{Z}_l)$ and $(\bar{A}_h, \bar{Z}_h)$ of the two maxima of the two-humped surface $y(A, Z)$ on the A, Z plane.

IV. CONFRONTATION WITH THE WILKINS-STEINBERG MODEL

We found the Wilkins-Steinberg model[11, 12] successful in interpreting and reproducing the essential features of isotopic mass dispersion even where discontinuity is present. These authors have shown that the formation probabilities of fragment pairs are strongly influenced by sizable deformed-shell corrections for neutrons. Hence, it would be of interest to calculate mass dispersions by using the model[12] for comparison, and to discuss the influence of neutron shell effect on the mass dispersion discontinuity on the basis of the neutron-shell correction vs the deformation and neutron number map of the model.

The mass dispersions in terms of product mass number for $Z = 34$, 36, 41, 42, 50, 51, 54, and 56 in thermal-neutron-induced fission of ^{235}U have been calculated by using the relative independent fragment yields $Y_r(Z, A')$ for mass numbers A', kindly communicated by Wilkins and Steinberg.[13]

A product of mass number $A = A' - n$ is formed by evaporation of n neutrons from the fragment. The actual neutron evaporation probabilities $P_n(\bar{\nu})$ are estimated by assuming a Gaussian[14] distribution around the most probable evaporated neutron number $\bar{\nu}(Z, A')$ defined by

$$\bar{\nu}(Z, A') = \frac{E_{\text{def}} + E_{\text{int}}}{E_k + E_b} ,$$

where E_{def} is the deformation energy, E_{int} is the intrinsic energy, E_k is the average neutron kinetic energy, and E_b is the neutron binding energy. The values of E_{def} and E_{int} have been determined from the model.[13] A plot of E_{def} vs deformation parameter was used to determine the former from the average deformation. The average deformations were calculated from the most probable deformations (β_l and β_h) listed for the light and heavy

TABLE IV. The isotopic mass dispersion parameters for thermal-neutron fission of ^{235}U, calculated by using the Wilkins-Steinberg model (Refs. 12 and 13) and the recommended data (Refs. 2 and 3). A_p is the most probable mass, c_1 and c_2 are the width parameters for the left and right branches of the dispersion.

	Parameters from fission yield data						Parameters from the		
	Based on the Meek-Rider report (Ref. 2)			Based on Wolfsberg's data (Ref. 3)			Wilkins-Steinberg model		
Z	c_1	c_2	A_p	c_1	c_2	A_p	c_1	c_2	A_p
36	4.6	4.1	90.227	4.1	4.4	90.150	3.8	3.4	91.247
38	4.5	5.1	94.745	4.5	5.2	94.788	4.5	2.7	94.890
41	4.8	4.6	101.898	4.5	4.5	101.974	4.2	6.9	100.466
42	3.8	4.8	103.696	3.7	5.1	103.674	n.G.	13.9	103.019
50	5.3	2.9	130.488	n.G.[a]	2.9	130.550	n.G.	3.0	129.971
51	4.1	3.0	132.250	5.0	3.2	132.244	7.3	4.4	131.202
54	4.5	4.6	138.522	4.4	4.8	138.500	3.2	3.9	137.798
56	4.7	3.7	143.285	4.4	3.9	143.246	4.4	4.2	141.327

[a] n.G. : non-Gaussian.

fragments, respectively, by examining how the potential surfaces for neutron- and proton-shell corrections look at different deformations. For simplicity, a constant value of 3 MeV may be used for E_{int}. Similarly, the values of 2 and 6 MeV were used for E_k and E_b, respectively.

The relative yield $y_{rn}(Z,A)$ of a product formed from a parent of mass number A' is $y_{rn}(Z,A) = Y_r(Z,A')P_n(\bar{\nu})$. Hence, the total independent relative yield of a product formed by all contributions will be $y_r(Z,A) = \sum_n y_{rn}(Z,A)$. Now, normalization $P_Z(A) = y_r(Z,A)/\sum_r y_r(Z,A)$ yields the $P_Z(A)$ values which then were treated by the "minimum systematic variance" technique as explained above.

Table IV shows that the dispersions calculated by the Wilkins-Steinberg model reproduce quite well both their Gaussian and discontinuous features. It should be noted that the nature of a dispersion (continuous or discontinuous) depends primarily on the difference Δc between the width parameters of the Gaussian branches rather than their absolute values. Inspection of Table IV along with the mentioned argument shows that the dispersions calculated by using the Wilkins-Steinberg model are in reasonable agreement with those obtained from recommended data (especially for the heavy group). Disagreement was observed only for $Z = 38$ and $Z = 41$, where the model predicts discontinuous dispersions, whereas the recommended data predict continuous ones. The inadequacy of our knowledge about the estimation of neutron-emission probability might be responsible for these discrepancies. However, the dispersion parameters for $Z = 41$, calculated from the model fit better the complementarity requirement [statement (4)].

Finally, the model's predictions[12] of strong neutron-shell regions at $N \approx 82$ (spherical) and $N \approx 88$ (deformed, $\beta = 0.65$), and of higher formation probabilities for fragments born in these regions are in good agreement with the results arrived at in statement (6) above (Figs. 2 and 3).

The authors are grateful to Dr. E. P. Steinberg and his associates for kindly communicating to them the manuscript of their paper (Ref. 12) prior to publication.

[1] M. Talât-Erben and Binay Dagsoz (Güven), Phys. Rev. C 2, 2403 (1970).
[2] M. E. Meek and B. F. Rider, Vallecitos Nuclear Center Report No. NEDO-121554-1, 1974 (unpublished).
[3] K. Wolfsberg, Los Alamos Scientific Laboratory Report No. LA-5553-MS, 1974 (unpublished).
[4] H. N. Erten, Inaugural Docentship thesis, Middle East Technical University, Ankara, 1975 (unpublished).
[5] M. Talât-Erben and Binay Güven, Phys. Rev. 129, 1762 (1963).
[6] M. Talât-Erben, Eurochemic Technical Report No. E. T. R., 114, 1961 (unpublished).
[7] F. Sheid, *Theory and Problems of Numerical Analysis* (McGraw-Hill, New York, 1968), p. 296 *et seq.*
[8] R. K. Tokay, Ph.D. thesis, Technical University of Istanbul, Istanbul, 1977 (unpublished).
[9] V. M. Strutinsky, Nucl. Phys. A95, 420 (1967).
[10] H. B. Levy and D. R. Nethaway, Report Nos. UCRL-6948 and Chem. UC-4, 1962 (unpublished).
[11] B. D. Wilkins and E. P. Steinberg, Phys. Lett. 42B, 141 (1972).
[12] B. D. Wilkins, E. P. Steinberg, and R. R. Chasman, Phys. Rev. C 14, 1836 (1976).
[13] E. P. Steinberg, private communication.
[14] J. Terrell, in *Proceedings of the International Atomic Energy Agency Symposium on the Physics and Chemistry of Fission, Salzburg, 1965* (IAEA, Vienna, 1965), Vol. 2, p. 3.